Well-Posed Initial-Boundary Evolution in General Relativity

Béla Szilágyi[1] , Jeffrey Winicour[1,2]

[1] *Department of Physics and Astronomy*
University of Pittsburgh, Pittsburgh, PA 15260, USA
[2] *Max-Planck-Institut für Gravitationsphysik, Albert-Einstein-Institut,*
14476 Golm, Germany

Maximally dissipative boundary conditions are applied to the initial-boundary value problem for Einstein's equations in harmonic coordinates to show that it is well-posed for homogeneous boundary data and for boundary data that is small in a linearized sense. The method is implemented as a nonlinear evolution code which satisfies convergence tests in the nonlinear regime and is stable in the weak field regime. A linearized version has been stably matched to a characteristic code to compute the gravitational waveform radiated to infinity.

The waveform emitted in the inspiral and merger of a relativistic binary is theoretical input crucial to the success of the fledgling gravitational wave observatories. A computational approach is necessary to treat the highly nonlinear regime of a black hole or neutron star collision. Developing this computational ability has been the objective of the Binary Black Hole (BBH) Grand Challenge [1] and other world wide efforts. The Grand Challenge based a Cauchy evolution code on the Arnowitt-Deser-Misner (ADM) [2] formulation of Einstein's equations. Exponentially growing instabilities encountered with that code have been traced to improper boundary conditions [3]. (Even in the absence of boundaries, an ADM system linearized off a Minkowski metric has a power law instability [4]; this triggers an exponential instability when the background Minkowski metric is treated in non-Cartesian, e.g. spherical, coordinates.) Other groups have encountered difficulties in treating boundaries (see [5] for a recent discussion) and the working practice is to forestall problems by placing the outer boundary far from the region of physical interest (see e.g. [6]) or compactify the spacetime (see e.g. [7]).

This deficiency extends beyond numerical relativity to a lack of analytic understanding of the initial-boundary value problem (IBVP) for general relativity. The local version of the IBVP is schematically represented in Fig. 1. Given Cauchy data on a spacelike hypersurface $\mathcal{S}$ and boundary data on a timelike hypersurface $\mathcal{B}$, the problem is to determine a solution in the appropriate domain of dependence. Whereas there is considerable mathematical understanding of the gravitational initial value problem (for reviews see [8]), until recently the IBVP has received little attention (see e.g. [9,10]). Indeed, only relatively recently has the method of maximally dissipative boundary conditions [11,12] been extended to the nonlinear IBVP with boundaries containing characteristics [13,14], such as occurs in symmetric hyperbolic formulations of general relativity. Friedrich and Nagy [10] have applied these methods to give the first demonstration of a well-posed IBVP for Einstein's equations. The Friedrich-Nagy work is of seminal importance for introducing the maximally dissipative technique into general relativity. Their formulation, which uses an orthonormal tetrad, the connection and the curvature tensor as evolution variables, is quite different from the metric formulations implemented in current codes designed to tackle the BBH problem. Although it is not apparent how to apply the details of the Friedrich-Nagy work to other formalisms, the general principles can be carried over provided Einstein's equations are formulated in the symmetric hyperbolic form

$$\sum_\alpha A^\alpha(u)\partial_\alpha u = S(u) \qquad (0.1)$$

with coordinates $x^\alpha = (t, x, y, z) = (t, x^i)$ and evolution variables $u = (u_1, ..., u_N)$, where A^α are $N \times N$ symmetric matrices and A^t is positive-definite.

The simplest symmetric hyperbolic version of Einstein's equations employs harmonic coordinates satisfying $H^\alpha := \sqrt{-g}\Box x^\alpha = \partial_\beta(\sqrt{-g}g^{\alpha\beta}) = 0$, in which the well-posedness of the initial value problem was first established [15,16]. Well-posedness expresses the existence of a unique solution with continuous dependence on the data. In the nonlinear case, existence is only guaranteed for a short time, reflecting the possibility of singularity formation. Here we show how this approach (i) can be applied to the IBVP problem in harmonic coordinates, (ii) can be implemented as a robustly stable, convergent 3-dimensional nonlinear Cauchy evolution code and (iii) can be accurately matched, in the linearized approximation, to an exterior characteristic evolution code to provide the proper physical boundary condition for computing the waveform radiated to infinity by an isolated source. Reference [17] discusses the suitability of harmonic coordinates for numerical work and for simulating the approach to a curvature singularity.

We base the evolution on the metric density $\gamma^{\alpha\beta} = \sqrt{-g}g^{\alpha\beta}$, with $g = \det(\gamma^{\alpha\beta}) = \det(g_{\alpha\beta})$. As in Eq. (B.87) of Fock [18], we split the Einstein tensor into $G^{\alpha\beta} = \mathcal{E}^{\alpha\beta} + \frac{1}{2}g^{\alpha\beta}B - B^{\alpha\beta}$, where $B^{\alpha\beta} = -(-g)^{-1/2}\nabla^{(\alpha}H^{\beta)}$ vanishes when $H^\alpha = 0$, where

$$\mathcal{E}^{\alpha\beta} = \frac{1}{2g}\gamma^{\mu\nu}\partial_\mu\partial_\nu\gamma^{\alpha\beta} + S^{\alpha\beta} \qquad (0.2)$$

and where $S^{\alpha\beta}$ contains no second derivatives of the metric. When the harmonic conditions $H^\alpha = 0$ are

satisfied, the reduced Einstein equations $\mathcal{E}^{\alpha\beta} = 0$ have principal part which is governed by the wave operator $\gamma^{\mu\nu}\partial_\mu\partial_\nu$. In terms of the evolution variables $u = (\gamma^{\alpha\beta}, \mathcal{T}^{\alpha\beta}, \mathcal{X}^{\alpha\beta}, \mathcal{Y}^{\alpha\beta}, \mathcal{Z}^{\alpha\beta})$, where $\mathcal{T}^{\alpha\beta} = \partial_t\gamma^{\alpha\beta}$, $\mathcal{X}^{\alpha\beta} = \partial_x\gamma^{\alpha\beta}$, $\mathcal{Y}^{\alpha\beta} = \partial_y\gamma^{\alpha\beta}$ and $\mathcal{Z}^{\alpha\beta} = \partial_z\gamma^{\alpha\beta}$, we put these wave equations in symmetric hyperbolic form (0.1) by a standard construction [19].

We adapt the harmonic coordinates to the boundary so that the evolution region lies in $z < 0$, with the boundary fixed at $z = 0$ in the numerical grid. We write $x^\alpha = (x^a, z) = (t, x, y, z)$ to denote coordinates adapted to the boundary, so that $x^\alpha = (x^a, z) = (t, x^i)$ depending whether the Latin index is near the beginning or end of the alphabet. We further adapt the coordinates so that $\gamma^{za}|_\mathcal{B} = 0$ (and hence $\mathcal{T}^{za}|_\mathcal{B} = 0$). For any timelike $\mathcal{B}$, these harmonic *gauge* conditions can be satisfied and they are assumed throughout the following discussion.

We base the well-posedness of the homogeneous IBVP on Theorems 2.1 and 2.2 of Secchi [14], which require that u satisfy a boundary condition of the form $Mu = 0$, where M is a matrix independent of u and of maximal rank such that the normal flux $\mathcal{F}^z = (u, A^z u)$ associated with an energy norm be non-negative. Secchi's theorems include the present case where the boundary is "characteristic with constant rank", i.e. A^z has a fixed number of 0 eigenvalues. The above gauge conditions considerably simplify this maximally dissipative condition for the reduced system $\mathcal{E}^{\alpha\beta} = 0$. The boundary matrix takes the form $A^z = \gamma^{zz}C$, where C is a constant matrix, and the flux inequality reduces to

$$\mathcal{F}^z = -\sum_{\alpha,\beta} \mathcal{T}^{\alpha\beta}\mathcal{Z}^{\alpha\beta} \geq 0. \tag{0.3}$$

Here $\mathcal{F}^z$ is identical to the standard energy flux for the sum of 10 independent scalar fields. This requirement can be satisfied in many ways, e.g. by combinations of the homogeneous Dirichlet boundary condition $\partial_t\gamma^{\alpha\beta} = \mathcal{T}^{\alpha\beta} = 0$, the homogeneous Neumann condition $\partial_z\gamma^{\alpha\beta} = \mathcal{Z}^{\alpha\beta} = 0$ and the homogeneous Sommerfeld condition $(\partial_t + \partial_z)\gamma^{\alpha\beta} = \mathcal{T}^{\alpha\beta} + \mathcal{Z}^{\alpha\beta} = 0$ on the various field components. All these boundary conditions have the required form $Mu = 0$. The maximality of the rank of M ensures that boundary conditions only be applied to variables propagating along characteristics entering the evolution region from the exterior [20]. For instance, assignment of a boundary condition to the variable $\mathcal{T}^{\alpha\beta} - \mathcal{Z}^{\alpha\beta}$, which propagates from the interior toward the boundary, would violate (0.3).

Whereas the well-posedness of the IBVP for the reduced system can be accomplished by a variety of boundary conditions, it can only be established for the full system in a limited sense. The Bianchi identities and reduced equations imply $\nabla_\mu(B^{\mu\nu} - \frac{1}{2}g^{\mu\nu}B) = 0$, which has the explicit form

$$\gamma^{\mu\nu}\partial_\mu\partial_\nu H^\alpha + C_\nu^{\alpha\mu}\partial_\mu H^\nu + D_\nu^\alpha H^\nu = 0, \tag{0.4}$$

where $C_\nu^{\alpha\mu}$ and D_ν^α depend algebraically on u and H^α. Thus H^α obeys a symmetric hyperbolic equation of the

form (0.1). Harmonic Cauchy data satisfying the Hamiltonian and momentum constraints and $H^\alpha = 0$ also satisfy $\partial_t H^\alpha = 0$ on $\mathcal{S}$ by virtue of the reduced equations, so that uniqueness guarantees $H^\alpha = 0$ in the domain of dependence $\mathcal{D}_1$ (see Fig. 1) and hence the well-posedness of the Cauchy problem for the full system. To extend well-posedness to the homogeneous IBVP, i.e. to include region $\mathcal{D}_2$, we impose boundary conditions for the reduced system that imply the homogeneous boundary conditions $H^z = 0$ and $\partial_z H^a = 0$ for the harmonic constraints. Combined with the gauge condition $\gamma^{za} = 0$, the condition $H^z := \partial_b\gamma^{zb} + \partial_z\gamma^{zz} = 0$ requires the Neumann boundary condition $Z^{zz} = 0$. We also impose the homogeneous Neumann boundary conditions $\mathcal{Z}^{ab} = 0$ so that $\partial_z H^a := \partial_b Z^{ab} + \partial_z^2\gamma^{az} = 0$ requires $\partial_z^2\gamma^{az} = 0$ at the boundary. Remarkably, subject to the above conditions, the reduced equation $\mathcal{E}^{az} = 0$ implies $\partial_z^2\gamma^{az} = 0$ at the boundary! Underlying this result is that $S^{az} = 0$ at the boundary due to the local reflection symmetry implied by the above conditions. This establishes the maximally dissipative boundary conditions $H^z = \partial_z H^a = 0$ for the constraint propagation equations (0.4) which ensure that the full Einstein system is satisfied.

In practice, homogeneous boundary conditions do not correspond to a given physical problem, e.g. homogeneous Neumann data at the end of a string lead to a free endpoint whereas the the endpoint might be undergoing a forced oscillation requiring inhomogeneous data. This flexibility is supplied within the maximally dissipative formalism by the ability to extend the homogeneous boundary condition $Mu = 0$ to the inhomogeneous form $M(x^a)(u - q(x^a)) = 0$ [10]. This preserves the well-posedness of the IBVP for the reduced system with inhomogeneous Neumann data $\mathcal{Z}^{zz} = q^{zz}$ and $\mathcal{Z}^{ab} = q^{ab}$. For the full system, the gauge condition $\gamma^{za} = 0$ and the boundary constraint $H^z = 0$ forces $q^{zz} = 0$. Next, $\partial_z H^a = 0$ implies

$$D_a(\mathcal{Z}^{ab}/\sqrt{-g^{zz}/g}) = 0, \tag{0.5}$$

where D_a is the connection intrinsic to the boundary. The appearance of the metric and D_a in Eq. (0.5) introduces u-dependence in the boundary data so that Secchi's theorems do not apply. However, the theory does apply to boundary data δq^{ab} linearized off a nonlinear solution with homogeneous data, either exact or generated numerically. Then Eq. (0.5) has the form

$$\partial_b\delta q^{ab} + F_{bc}^a(x^d)\delta q^{bc} = 0, \tag{0.6}$$

where $F_{bc}^a(x^d)$ is explicitly known via the metric and connection of the homogeneous solution. The principal part of Eq. (0.6) is identical to the analogous equation in the linearized version of the harmonic IBVP treated in Ref. [21]. In terms of the coordinates $x^a = (t, x^A) = (t, x, y)$ on the boundary, a simple transformation of variables (see [21]) recasts Eq. (0.6) as a symmetric hyperbolic system of equations for $\phi = \frac{1}{2}\delta_{AB}\delta q^{AB}$ and

$y^A = \delta q^{tA}$. (Here δ_{AB} is the Kronecker delta.) This system uniquely determines ϕ and y^A in terms of their initial values and the 3 pieces of free boundary data $y^{AB} = \delta q^{AB} + \delta^{AB}(\delta q^{tt} - \delta_{CD}\delta q^{CD})$. (This in accord with Ref. [10], although there is no direct correspondence with the three free pieces of boundary data in [10]). Since only coordinate conditions have been imposed here, the only restriction on physical generality is the linearity of the boundary data.

The IBVP also requires consistency between the Cauchy data and boundary data at $\mathcal{S} \cup \mathcal{B}$, which determines the degree of differentiability of the solution [14]. As in the string example, consistent homogeneous Neumann boundary data and Cauchy data imply a virtual reflection symmetry across the boundary, which is broken in the inhomogeneous case. Although the IBVP is well-posed for the reduced system and for the constrained system with boundary data linearized about the homogeneous case, no available theorems guarantee well-posedness for the constrained inhomogeneous case. In this respect, the analytic underpinnings are not as general as the Friedrich-Nagy formulation. Numerical simulations are necessary to shed further light on this question. The key feature of our formulation is that *if a solution exists, as provided by a convergent numerical simulation, then it necessarily satisfies the constraints*, since the constraint propagation equation (0.4) is then satisfied with maximally dissipative, homogeneous boundary data. In the strong field convergence tests described below, exact solutions provide the Cauchy and boundary data.

In constructing a code to demonstrate these results, we take considerable liberty with the symmetric hyperbolic formalism. In particular, we use the second differential order form of the equations based upon the 10 variables $\gamma^{\alpha\beta}$ rather than the 50 first order variables u; we use a cubic boundary aligned with Cartesian coordinates, although the mathematical theorems only apply to smooth boundaries; and we replace the gauge condition $\gamma^{za} = 0$ by $\gamma^{za} = q^a(x^b)\gamma^{zz}$, where $q^a = \partial_z x^a|_{\mathcal{B}}$ is the free Neumann boundary data in the transformation to a general harmonic coordinate system satisfying $\Box x^a = 0$. The harmonic boundary constraint $H^z = 0$ now implies $q^{zz} = -\partial_a(q^a\gamma^{zz})|_{\mathcal{B}}$ and the constraint $\partial_z H^a = 0$ again determines ϕ and y^A in terms of the free boundary data (q^a, y^{AB}), now through a symmetric hyperbolic system obtained from adding source terms arising from $q^a \neq 0$ to the right hand side of Eq. (0.5). We use the finite difference techniques described in [21], where robust stability and convergence of a linearized harmonic code was demonstrated. In the linearized theory, the decoupling of the metric components gives more flexibility in formulating a well-posed IBVP. The linearized harmonic code could be consistently implemented with Dirichlet boundary conditions, in which case it ran stably for 2000 crossing times even with a piecewise-cubic spherical boundary cut out of the Cartesian grid. However, we have not found a well-posed version of the nonlinear theory that

avoids Neumann boundary conditions and the associated numerical complications which we describe below.

We tested robust stability [23] of the nonlinear code by initializing the evolution with random, constraint violating initial data $\gamma^{\alpha\beta} = \eta^{\alpha\beta} + \epsilon^{\alpha\beta}$ and by assigning random boundary data $q(x^a) = \epsilon$ at each point of the cubic grid boundary, with the ϵ's random numbers in the range $(-10^{-10}, 10^{-10})$. (Although differing from the standard numerical definition of stability related to convergence, robust stability is computationally practical for revealing short wavelength instabilities.) Under these conditions, the noise in the nonlinear code grows linearly at the same rate for 2000 crossing times for both the 48^3 and 72^3 grids. We tested convergence in the nonlinear regime using a gauge-wave generated by the harmonic coordinate transformation $(x, y) = x^B \to x^B + a^B \sin\left[2\pi\left(\sqrt{3}t + x + y + z\right)\right]$ acting on the Minkowski metric, with $a^x = 0.06\,A$, $a^y = 0.04\,A$. The resulting gauge-wave has amplitude $||g^{\alpha\beta} - \eta^{\alpha\beta}||_\infty \approx A$. We use periodicity in the (x, y) plane to evolve with smooth toroidal boundaries at $z = \pm 1/2$. Second-order convergence in the non-linear regime was confirmed with the amplitude $A = 10^{-1}$. Figures 2 demonstrates the convergence of the solution and Fig. 3 shows the absence of anomalous boundary error. Error arising from the application of Neumann boundary conditions eventually triggers a nonlinear instability, which occurs after 30 crossing times with the 120^3 grid. Runs with the amplitude $A = 10^{-3}$ were carried out on the 80^3 grid for 300 crossing times without encountering the above nonlinear instability (see Figure 2). In the case of a cubic boundary, the nonlinear code cleanly propagates a physical pulse with amplitude 10^{-7} that corresponds to an exact linearized solution; but, for a gauge-wave of amplitude $A = 10^{-3}$, substantial error arises at the edges and corners due to our present method of applying Neumann boundary conditions and leads to an instability after 60 crossing times.

The physically proper boundary data for a given problem is a separate and difficult problem for nonlinear systems. One approach is to supply $q(x^a)$ by Cauchy-characteristic matching (CCM) in which an interior Cauchy evolution with cubic boundary is matched to an exterior characteristic evolution on a sequence of outgoing null cones extending to infinity (for a review see [22]). In simulations of a nonlinear scalar wave with periodic source, CCM was demonstrated to compute the radiated waveform more efficiently and accurately than existing artificial boundary conditions on a large but finite boundary. [24] Previous attempts at CCM in the gravitational case were plagued by boundary induced instabilities growing on a scale of 10 to 20 grid crossing times. Although stable behavior of the Cauchy boundary is only *a necessary but not a sufficient* condition for CCM, tests carried out with a linearized harmonic Cauchy code with a well-posed IBVP matched to a linearized characteristic code show no instabilities.

In the tests of CCM, the linearized Cauchy code was supplied outer boundary data q in Sommerfeld form by the exterior characteristic evolution and boundary data for the characteristic code was supplied on an interior spherical boundary by the Cauchy evolution. Robust stability for 2000 crossing times on a Cauchy grid of 45^3 was confirmed. For a linearized wave pulse, Figure 4 shows a sequence of profiles of the metric component γ^{xy} propagating cleanly through the spherical boundary as the wave pass to the characteristic grid, where it is propagated to infinity. Further details and tests of CCM and the question of its extension to the nonlinear theory will be reported elsewhere.

At present, the major limitation in the nonlinear code stems from the difficulty in handling large values of γ^{tz} at the boundary. This is evidenced by numerical experiments with the manifestly well-posed IBVP consisting of a scalar wave propagating between smooth toroidal boundaries according to the flat-space wave equation

$$\left(-\partial_t^2 - 2v\partial_t\partial_z + \partial_x^2 + \partial_y^2 + (1-v^2)\partial_z^2 \right)\Phi = 0,$$

which arises from the transformation $z \to z + vt$ on standard inertial coordinates. The value of γ^{tz} represents the velocity of the boundary relative to observers at rest with respect to the Cauchy slicing. For the flat space wave equation in second order form, there have apparently been no studies of numerical algorithms which apply Neumann boundary conditions to such moving boundaries. In fact, only very recently has there been a thorough treatment of Neumann boundary conditions for the the flat space wave equation with a stationary (but curvilinear) boundary [25]. This treatment uses Neumann data to update the field at a boundary point at the current time step by a one-sided finite difference approximation for the normal derivative. Such stencils for approximating normal derivatives apply only when the normal direction is tangent to the Cauchy slicing, i.e. when $g^{tz}|_{\mathcal{B}} = 0$. The general case in which $g^{tz}|_{\mathcal{B}} \neq 0$ requires a more complicated stencil involving interior points to the future or past of the current time step. We have developed a new approach which successfully handles this general case for the above scalar wave test problem but requires further refinement to handle boundaries with edges and corners before it can be implemented in the gravitational code.

[1] S. Brandt et al, *Phys. Rev. Lett.*, **85**, 5496 (2000).

[2] R. Arnowitt, S. Deser and C. Misner, in *Gravitation: An Introduction to Current Research*, ed. L. Witten (Wiley, NY, 1962).

[3] B. Szilágyi, R. Gómez, N. T. Bishop and J. Winicour, *Phys. Rev. D*, **62**, 104006 (2000).

[4] G. Calabrese, J. Pullin, O. Sarbach and M. Tiglio, *Phys. Rev. D*, **66**, 041501 (2002).

[5] G. Calabrese, L. Lehner and M. Tiglio, *Phys. Rev. D*, **65**, 104031 (2002).

[6] R. L. Marsa and M. W. Choptuik, *Phys. Rev. D*, **54**, 4929 (1996).

[7] S. Husa, *Problems and Successes in the Numerical Approach to the Conformal Field Equations*, in *The Conformal Structure of Spacetimes: Geometry, Analysis, Numerics*, ed. J. Frauendiener and H. Friedrich, Lecture Notes in Physics 604 (Springer, New York, 2002).

[8] O. Reula, *Living. Rev. Rel.*, **1**, 3 (1998); H. Friedrich and A. Rendall, in *Einstein's Equations and Their Physical Implications*, edited by B. Schmidt (Springer, New York, 2000); A, Rendall, *Living. Rev. Rel.*, **4**, 1 (2001).

[9] J. M.Stewart, *Class. Quantum Grav.*, **15**, 2865 (1998).

[10] H. Friedrich and G. Nagy, *Commun. Math. Phys.*, **201**, 619 (1999).

[11] K. O. Friedrichs, *Comm. Pure Appl. Math.*, **11**, 333 (1958).

[12] P. D. Lax and R. S. Phillips, *Comm. Pure Appl. Math.*, **13**, 427 (1960).

[13] J. Rauch, *Trans. Am. Math. Soc.*, **291**, 167 (1985).

[14] P. Secchi, *Arch. Rational Mech. Anal.*, **134**, 155 (1996).

[15] Y. Foures-Bruhat, *Acta. Math.*, **88**, 141 (1955).

[16] A. E. Fisher and J. E. Marsden, *Comm. Math. Phys.*, **28**, 1 (1972).

[17] D. Garfinkle, *Phys.Rev.*, **D65**, 044029 (2002).

[18] V. Fock,*The Theory of Space, Time and Gravitation*, p. 392 (MacMillan, New York, 1964).

[19] R. Courant and D. Hilbert, *Methods of Mathematical Physics, Vol. II*, p. 594 (Interscience, NY, 1962).

[20] B. Gustafsson, H.-O. Kreiss and J. Oliger, *Time Dependent Problems and Difference Methods* (Wiley, NY, 1995).

[21] B. Szilágyi, B. Schmidt and J. Winicour, *Phys. Rev.*, **D65**, 064015 (2002).

[22] J. Winicour, *Living. Rev. Rel.*, **4**, 3 (2001).

[23] The robust stability test has been extended to include dependence on grid size in "Toward standard testbeds for numerical relativity", M. Alcubierre *et al*, gr-qc/0305023.

[24] N. T. Bishop et al, *J. Comp. Phys.*, **136**, 140 (1997).

[25] H.-O. Kreiss, N. A. Petersson and J. Yström, *SIAM Journal on Numerical Analysis*, **40**, No. 5, pp 1940-1967 (2002).
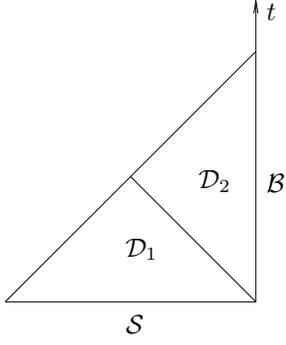
FIG. 1. Schematic representation of the domain of dependence $\mathcal{D}_1$ of the initial value problem and the domain of dependence $\mathcal{D}_1 \cup \mathcal{D}_2$ of the IBVP.
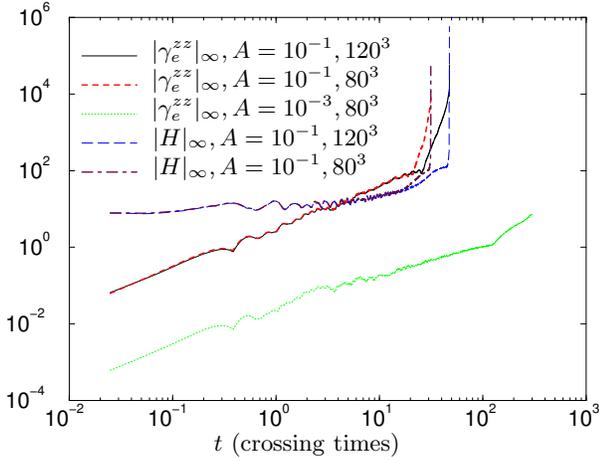

FIG. 2. The L_∞ norm of the finite-difference error $\gamma_e^{zz} = \gamma_{ana}^{zz} - \gamma_{num}^{zz}$, rescaled by a factor of $1/\Delta^2$, for a gauge-wave. The upper two (mostly overlapping) curves demonstrate convergence to the analytic solution for a wave with amplitude $A = 10^{-1}$ with gridsizes 80^3 and 120^3. We also plot $|H|_\infty$, the L_∞ norm of $\sqrt{(H^t)^2 + \delta_{ij}H^i H^j}$, to demonstrate that convergence of the harmonic constraints is enforced by the boundary conditions. The lower curve represents evolution of the same gauge-wave with $A = 10^{-3}$ for 300 crossing times with gridsize 80^3.
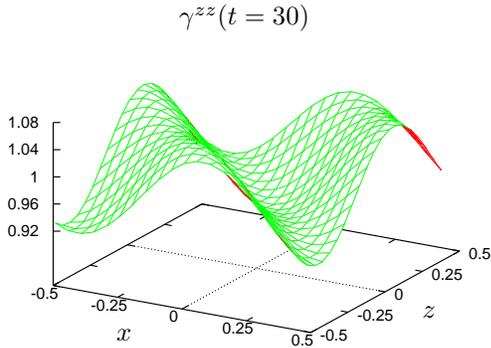

FIG. 3. A $y = 0$ slice of the metric component γ^{zz}, evolved for 30 crossing times, amplitude $A = 10^{-1}$, with a toroidal boundary in the (x, y) plane.

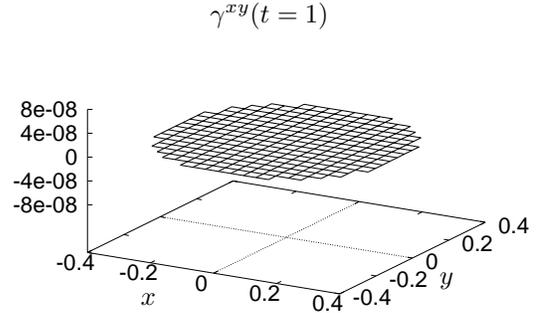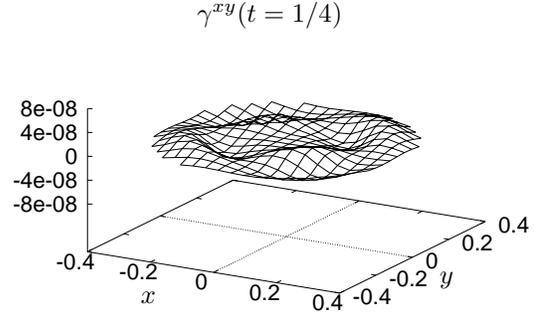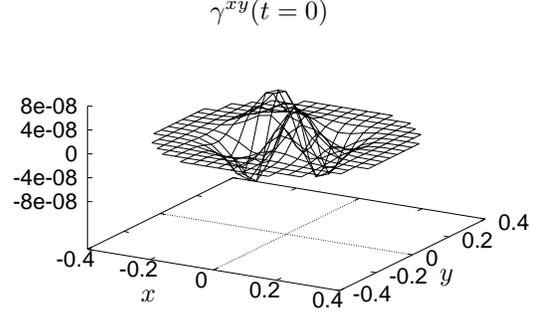FIG. 4. Sequence of $z = 0$ slices of the metric component γ^{xy}, evolved for one crossing time, with the linear matched Cauchy-characteristic code. In the last snapshot, the wave has propagated cleanly onto the characteristic grid.

5